



Characterizing deep-water oxygen variability and seafloor community responses using a novel autonomous lander

5 Natalya D. Gallo^{1,2,3}, Kevin Hardy⁴, Nicholas C. Wegner², Ashley Nicoll¹, Haleigh Yang⁵, Lisa A. Levin^{3,5}

¹Marine Biology Research Division, Scripps Institution of Oceanography, University of California San Diego, La Jolla, California 92093, USA

10 ²Fisheries Resources Division, Southwest Fisheries Science Center, NOAA Fisheries, 8901 La Jolla Shores Drive, La Jolla, CA 92037, USA

³Center for Marine Biodiversity and Conservation, Scripps Institution of Oceanography, University of California San Diego, La Jolla, California 92093, USA

⁴Global Ocean Design LLC, 7955 Silverton Avenue Suite 1208, San Diego, CA 92126, USA

15 ⁵Integrative Oceanography Division, Scripps Institution of Oceanography, University of California San Diego, La Jolla, California 92093, USA

Correspondence to: Natalya D. Gallo (ndgallo@ucsd.edu)

Abstract. Studies on the impacts of climate change typically focus on changes to mean conditions. However, animals live in temporally variable environments which give rise to different exposure histories that could affect sensitivities to climate change. Ocean deoxygenation has been observed in nearshore, upper-slope depths in the Southern California Bight, but how these changes compared to the magnitude of natural O₂ variability experienced by seafloor communities at short time-scales was unknown. We aimed to develop a low-cost and spatially flexible approach for studying nearshore, deep-sea ecosystems and monitoring deep-water oxygen variability and benthic community responses. Using a novel, autonomous hand-deployable Nanolander with an SBE MicroCAT and camera system, high-frequency environmental (O₂, T, pHest) and seafloor community data were collected at depths between 100-400 m off San Diego, CA to characterize: timescales of natural environmental variability, changes in O₂ variability with depth, and community responses to O₂ variability. Oxygen variability was strongly linked to tidal processes, and contrary to expectation, oxygen variability did not decline linearly with depth. Depths of 200 and 400 m showed especially high O₂ variability which may buffer communities at these depths to deoxygenation stress by exposing them to periods of relatively high O₂ conditions across short time-scales (daily and weekly). Despite experiencing high O₂ variability, seafloor communities showed limited responses to changing conditions at these shorter time-scales. Over 5-month timescales, some differences in seafloor communities may have been related to seasonal changes in the O₂ regime. Overall, we found lower oxygen conditions to be associated with a transition from fish-dominated to invertebrate-dominated communities, suggesting this taxonomic shift may be a useful ecological indicator of hypoxia. Due to their small size and ease of use with small boats, hand-deployable Nanolandings can serve as a powerful



35 capacity-building tool in data-poor regions for characterizing environmental variability and examining seafloor community
sensitivity to climate-driven changes.

1 Introduction

Natural environmental variability can affect the resilience or sensitivity of communities to climate change. Communities and species living in variable environments are often more tolerant of extreme conditions than communities
40 from environmentally constant areas (Bay and Palumbi 2014). In seasonally hypoxic Pacific fjords, temporal oxygen
variability influences seafloor community beta diversity patterns, and can allow certain species to survive even when average
oxygen conditions are below their critical oxygen thresholds (P_{crit}) (Chu et al. 2018). The anthropogenic signal of
deoxygenation also takes a longer time to emerge in systems with higher natural oxygen variability (Long et al. 2016,
Henson et al. 2017), such as Eastern Boundary Upwelling systems. Natural variability of dissolved oxygen at different time
45 scales is therefore an important environmental factor to consider when studying the impacts of deoxygenation on
communities.

While data on shallow-water O_2 and pH variability have proven valuable for interpreting faunal exposures
(Hofmann et al. 2011b, Frieder et al. 2012, Levin et al. 2015), high-frequency measurements are rare below inner shelf
depths. No published high-frequency deep-water O_2 or pH measurements are available for depths below 100 m in the
50 Southern California Bight (SCB). The California Cooperative Oceanic Fisheries Investigations (CalCOFI) long-term time
series provides quarterly measurements showing decreases in oxygen conditions from 1984 to 2006 of up to $2.1 \mu\text{mol kg}^{-1} \text{y}^{-1}$
in the SCB, with a mean decrease of 21% below the thermocline at 300 m (Bograd et al. 2008, 2015). However, similar low
oxygen levels were measured in the late 1950s and 60s (McClatchie et al. 2010). Notably, daily, weekly and even seasonal
low oxygen extreme events (e.g. Send and Nam 2012) are not captured by the quarterly CalCOFI sampling frequency. Due
55 to the physical oceanography and variable bathymetry of the SCB, nearshore deep-water areas on the shelf and slope may
experience high variability due to localized wind-driven upwelling events (Send and Nam 2012) and mixing from internal
waves (Nam and Send 2011). The California Undercurrent transports warm, saline, low-oxygen subtropical water northward
along the coast in the SCB and varies seasonally in strength, depth, and direction (Lynn and Simpson 1987), likely
contributing to deep-water O_2 variability.

60 Datasets on organismal and community responses to environmental variability are rare for the deep sea, however
those that exist are informative and illustrate a dynamic environment (Chu et al. 2018, Matabos et al. 2012). Studies from
NEPTUNE (the North-East Pacific Time-Series Undersea Networked Experiments) in B.C. Canada show that even at 800-
1000 m, fish behavior is linked to variations in environmental conditions across different temporal scales including day-night
and internal tide temporalizations (Doya et al. 2014) and seasonal cycles (Juniper et al. 2013). Combined high-frequency
65 quantitative sampling of environmental and biological data allows examination of which processes shape benthic
communities (Matabos et al. 2011, 2014).



Currently, tools for studying deep-water, seafloor ecosystems include deep-submergence vehicles (HOVs, AUVs, and ROVs), towed camera sleds, and trawls. These approaches typically require significant resource investment, and the use of large ships with winch capabilities. Moorings and cabled observatories are also very useful, however, are usually fixed to specific sites and are typically costly. Autonomous landers have several advantages for deep-sea research, such as lower cost combined with spatial flexibility. Unlike moorings or cabled observatories, small landers (< 2 m high) can easily be recovered using small boats and redeployed to new depths and locations (Priede and Bagley 2000, Jamieson 2016).

This study focuses on oxygen variability and community composition at depths between 100-400 m along the nearshore environment in the SCB. This depth zone is of interest because it encompasses the oxygen limited zone (OLZ) ($O_2 < 60 \mu\text{mol kg}^{-1}$ as defined in Gilly et al. 2013) and supports many important recreational and commercial fish species, including many species of slope rockfish (genus *Sebastes*), which may be vulnerable to deoxygenation (Keller et al. 2015, McClatchie et al. 2010). The OLZ is a transition zone above the oxygen minimum zone (OMZ, $O_2 < 22.5 \mu\text{mol kg}^{-1}$), where dissolved oxygen levels exclude hypoxia-intolerant species. The shallow upper OMZ boundaries likely experience more temporal variability than lower boundaries because upwelling is a generally shallow phenomenon (< 200 m) and these waters may be more biogeochemically responsive to changes in surface production. Thus, seafloor communities in the OLZ may be highly responsive to short-term and seasonal changes in oxygenation.

Upper slope depths on the US West Coast appear to be especially affected by global trends of oxygen loss (Levin 2018). Off Monterey Bay in Central California, depths between 100-350 m have seen declines in oxygen of $1.92 \mu\text{mol kg}^{-1} \text{ year}^{-1}$ between 1998-2013 (Ren et al. 2018). In the SCB, oxygen declines of $1-2 \mu\text{mol kg}^{-1} \text{ year}^{-1}$ have been reported by several studies over a period of ~30 years (Bograd et al. 2008, McClatchie et al. 2010, Meinvielle and Johnson 2013), with the largest relative changes occurring at 300 m (Bograd et al. 2008). The proposed mechanisms for observed oxygen loss include increased advection of and decreasing oxygen in Pacific Equatorial Water (PEW) (Meinvielle and Johnson 2013, Bograd et al. 2015, Ren et al. 2018) and increased respiration, which is suspected to contribute more to oxygen loss at shallower depths (< 150 m) (Booth et al. 2014, Bograd et al. 2015, Ren et al. 2018). Long term declines in pH and aragonite saturation state have been demonstrated for the California Current System over similar periods using ROMS simulations (Hauri et al. 2013). Understanding the superposition of these long-term trends on significant natural high frequency variability will be key to evaluating biotic responses.

The goals of this study are to: (i) increase sensor accessibility to nearshore deep-water ecosystems through the development and testing of a small autonomous Nanolander, (ii) characterize deep-water O_2 variability over hours, days, and weeks at upper slope depths in the SCB relative to mean deoxygenation trends over decades, and identify dominant timescales and depths of variability between 100-400 m, (iii) describe shelf and slope assemblages using the Nanolander camera system, and (iv) examine if and how the seafloor community responds to O_2 variability at short timescales (daily, weekly, seasonal) in terms of community composition and diversity.



2 Methods

100 2.1 Nanolander development and deployment

Autonomous landers have been used successfully to observe abyssal and deep-sea trench communities (e.g., Jamieson et al. 2011, Gallo et al. 2015), however, these landers were large and required a ship with an A-frame and winch to deploy and recover. For this study, the goal was to develop a deep-water lander that could easily be hand-deployed out of a small boat and that was capable of continuously collecting hydrographic and fish and invertebrate assemblage data from near the seafloor for several weeks at a time at water depths to 1000 m. With this goal in mind, the “Nanolander” *Deep Ocean Vehicle (DOV) BEEBE*, was developed and built (Global Ocean Design, San Diego, CA) (Fig. 1A). *DOV BEEBE* is named for William Beebe (1877-1962) who illuminated the deep-sea world during his Bathysphere dives (Beebe 1934).

DOV BEEBE stands 5.25 ft tall (1.6 m) and is 1.17 ft (36 cm) wide and 1.17 ft (36 cm) deep. The Nanolander frame is made of marine-grade high-density polyethylene (brand name “Starboard”) and reinforced with fiberglass pultruded channel and angle beams for structure, reducing in-water weight. Alloy 316 stainless steel fasteners hold the frame together. Within the frame sit three glass-filled polyamide trawl float spheres that are 10 inches (~25 cm) in diameter. These spheres are used for both buoyancy and instrument housing and are rated to 1000 m. When needed, additional smaller glass-filled polyamide spheres were used to increase buoyancy. When *DOV BEEBE* is deployed, the vertical distance from the base of the Nanolander to the seafloor is ~18 inches (~51 cm) (Fig. 1B). This distance is defined by the length of the anchor chain connecting the lander release system to the expendable iron anchor and may be shortened or lengthened.

All three main spheres of *DOV BEEBE* are used to support electronics and instrumentation required for deployment, data collection, and recovery. The upper sphere houses an Edgetech BART (Burnwire-Acoustic Release-Transponder) board, which is the prime means of communication with the Nanolander. A transducer is bounded to the exterior of the upper sphere, positioned to point upwards with a clear view to the surface. The Edgetech BART board has four pre-programmed commands which enable and disable acoustic responses, and initiate the burn command for recovery. An overboard transducer and an Edgetech deckbox are used to communicate acoustically with the upper sphere, and allow distance ranging on the Nanolander. The power supply for the BART board is housed in the upper sphere.

The middle sphere functions as a “battery pod” and houses the batteries and battery management system (BMS) that power the two external LED lights. The circuit engineered to power the LED lights consists of five components: Battery > Battery Management System (BMS) > Relay > LED Driver > LED lights. Rechargeable lithium-polymer batteries were used and are recharged through an external cable and charger system without having to open the middle sphere. For all but one deployment, a 30-ampere hour (Ah) battery stack was used to power the LED lights, which was composed of three 14.8v/10 Ah units. For the last deployment, power capacity was upgraded to 32 Ah by using two 14.8v/16 Ah batteries. In each case, each individual battery (10 or 16 Ah) had its own battery management system (BMS) with a low voltage cut-out (LVCO) to ensure that battery discharge never went below a critical threshold (12.0 v), which would damage the battery.



The relay and LED drivers are contained within the lower sphere, which houses all components of the camera system, and includes the viewport. The camera system uses a Mobius Action Camera with a time-lapse assembly, which was modified by Ronan Gray (SubAqua Imaging Systems, San Diego, CA) and William Hagey (Pisces Design, La Jolla, CA). The camera system has 14 different time-lapse options, including continuous video, time-lapse images, and time lapse video
135 at pre-programmed intervals. For these deployments, a sampling interval of 20 seconds of video every 20 minutes was used. A sealed magnetic switch triggers the camera system to begin programmed sampling at a pre-determined interval. An internal light-sensitive relay, pointed towards a camera indicator LED, triggers the external LED lights to power on. The two LED lights are attached to the body of the Nanolander and positioned on either side of the middle sphere. All spheres were sealed with a Deck Purge Box (Global Ocean Design, San Diego, CA) using a desiccant cartridge to remove moisture, and
140 were held together by a vacuum of ~12 psi.

Below the bottom camera sphere, *DOV BEEBE* has a mounted SBE 37-SMP-ODO instrument (Sea-Bird Scientific) housed within a titanium housing and rated to 7000 m. The MicroCAT CT(D)-DO is a highly accurate sensor designed for moorings and other long-duration, fixed-site deployments. It includes a conductivity, temperature, pressure, and SBE 63 optical dissolved oxygen sensor. Initial sensor accuracy is +/- 3 $\mu\text{mol kg}^{-1}$ for oxygen measurements, +/- 0.1% for pressure
145 measurements, +/- 0.002°C for temperature measurements, and +/- 0.0003 S m^{-1} for conductivity measurements, and drift is minimal. The SBE MicroCAT was programmed to take samples every 5 minutes for the length of the whole deployment.

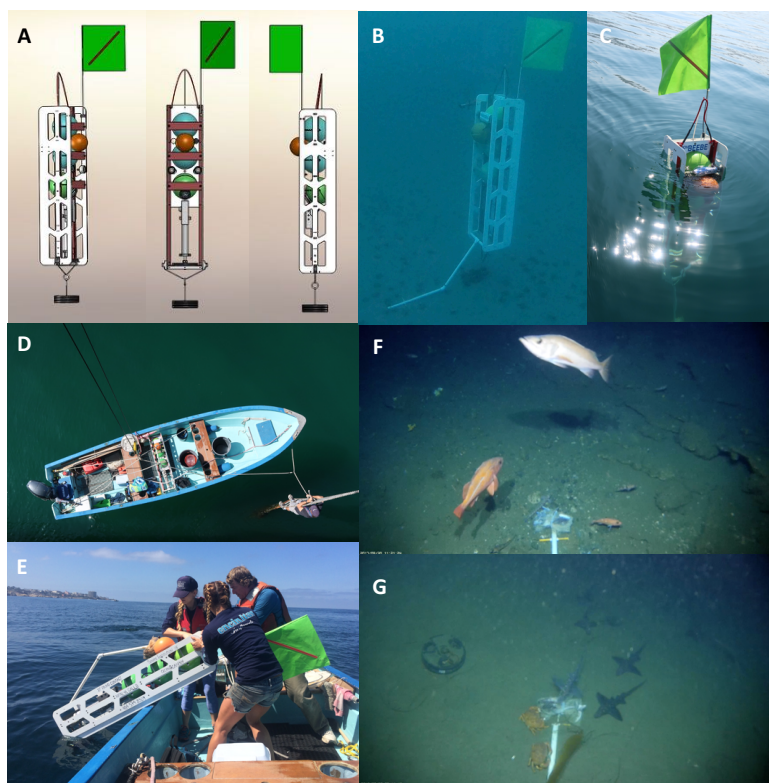
A drop-arm is mounted in front of *DOV BEEBE*, and is secured with a release during deployment. Initially a galvanic release was used, but a stack of 3-4 “Wint O Green” lifesavers was found to be more time-efficient. The drop-arm served three functions: it stabilized the Nanolander when exposed to current, it had a 6 inch (15.24 cm) cross-bar for visual
150 sizing reference, and it was used to attach bait for each deployment. The bait used was composed of an assortment of previously frozen demersal fishes that are part of the SCB upper margin demersal fish community. Bait was secured within a mesh cantaloupe bag and secured to the drop-arm with Zip-Ties for each deployment. All bait had been eaten by recovery.

DOV BEEBE is positively buoyant in water, and is deployed with 40 lbs of sacrificial iron weights. The weights are attached by a sliding link onto a metal chain, which is secured on each side to the base of the Nanolander using a burn wire.
155 Successful release of either burn wire allows the metal link to slide off the chain and drop the weights, releasing the Nanolander from the bottom. *DOV BEEBE*'s estimated descent rate is ~100 m per minute, and ascent rate is ~60 m per minute, following release of the weights. Once at the surface, *DOV BEEBE* floats ~1.5 feet (0.45 m) above the water and has a large flag, which assists with visual detection of the Nanolander (Fig. 1C).

Seven deployments were conducted during the study period, ranging from 15-35 days, and at targeted depths of
160 100-400 m (Table 1). Two early deployments (D200-LJ-1 and D200-LJ-2) were done near the Scripps Reserve off La Jolla, CA and five subsequent deployments (D100-DM-Fall, D200-DM, D300-DM, D400-DM, D100-DM-Spr) targeted a nearby rockfish habitat – the Del Mar Steeples Reef, CA. Environmental and camera-based community data were collected during six of the seven deployments; only environmental data are available from the first deployment (D200-LJ-1) due to a camera technical problem. We aimed to conduct repeat deployments at each site to capture seasonal differences between a period of



165 relaxed upwelling (fall/winter) and a period of strong upwelling (spring/summer), however full sampling was not feasible
due to time and equipment constraints. Consequently, only one repeat deployment is available for ~100 m at Del Mar
Steeple Reef (D100-DM-Fall and D100-DM-Spr).



170 **Figure 1:** *DOV BEEBE* is an autonomous, hand-deployable Nanolander capable of operating to 1000 m depth. It is outfitted with a
Seabird MicroCAT-ODO environmental sensor for collecting high-frequency measurements of near-seafloor temperature, oxygen,
salinity, and pressure, and a camera and light system for collecting videos of seafloor communities. The design for *DOV BEEBE* is
shown in (A), and *DOV BEEBE* is shown deployed at 30 m depth in (B), and floating at the surface in (C) prior to recovery.
BEEBE can easily be deployed by several people from a small boat (D, E). Examples of the field of view from the camera system
175 are shown in (F) from D100-DM-Fall at ~100 m off Del Mar Steeple Reef and in (G) from D200-LJ-2 at ~200 m near the Scripps
Reserve. The drop arm with the bait bag can be seen.

2.2 Characterizing environmental variability on the shelf and upper slope

Upon recovery of the Nanolander, time-series data from the MicroCAT were analyzed to assess how high-
frequency environmental variability (O_2 , T, salinity) changes with depth. Since partial pressure of oxygen may be more
180 biologically meaningful than oxygen concentration for understanding animal exposures to oxygen, we also calculated



oxygen partial pressure as in Hofmann et al. (2011a). Oxygen and pH naturally co-vary along the continental margin driven by respiration. To examine variability of carbonate chemistry parameters, pH, Ω_{arag} , and Ω_{calc} were estimated using empirical equations derived for this region in Alin et al. (2012).

The mean and ranges of environmental conditions were compared across depths and deployments to characterize differences in environmental variability that seafloor communities are exposed to over short time-scales. Probability density distributions of environmental conditions were used to visualize differences in environmental conditions for each deployment. The coefficient of variation (CV) (i.e. the ratio of the standard deviation to the mean) was calculated for environmental variables for each deployment as a standardized measure of dispersion and compared across deployments and depths. Additionally, the percent of measurements in which conditions were hypoxic ($\text{O}_2 < 60 \mu\text{mol kg}^{-1}$), severely hypoxic ($\text{O}_2 < 22.5 \mu\text{mol kg}^{-1}$), or undersaturated with respect to aragonite ($\Omega_{\text{arag}} < 1$) or calcite ($\Omega_{\text{calc}} < 1$) was determined for each deployment.

Previous studies have found that changes in oxygen and pH in the Southern California Bight are associated with changes in the volume of Pacific Equatorial Water (PEW) transported in the California Undercurrent (Bograd et al. 2015, Nam et al. 2015). PEW is characterized by low oxygen, warm, and high salinity conditions. Spiciness, which is a state variable that is conserved along isopycnal surfaces (Flament 2002), can be used as a tracer for PEW (Nam et al. 2015). We calculated spiciness using the “oce” R package (Kelley and Richards 2017) and examined how oxygen concentration varies with temperature and spiciness across depths and deployments.

To identify the dominant timescale of variability for oxygen, a spectral analysis was conducted as in Frieder et al. (2012) on the oxygen time series for each deployment. To look at diurnal and semidiurnal patterns, one day was used as the unit of time, and the number of observations based on the sampling frequency, was 288. Spectral analyses were conducted on detrended time series using a fast fourier transform. Results were displayed using a periodogram and the period of the dominant signal was compared across deployments. The oxygen time series for each deployment was also decomposed to look at the trend, daily, and random signals that contribute to the overall data patterns.

2.3 Assessing community responses to oxygen variability

Video segments recorded by the camera system were annotated to analyze if and how seafloor communities differ with respect to environmental conditions. A total of 4,293 20-second video segments were collected and annotated in total. For each 20-second video, both invertebrates and vertebrates within the frame of view were identified to lowest taxonomic level and counted.

Since visibility was impaired during certain deployments due to high turbidity, each video clip was categorized by visibility quality using the following categories: 1 (can see the bottom, good visibility), 2 (can only see the drop-arm, poor visibility), or 3 (drop-arm can no longer be seen, no visibility). Only samples with a visibility category of 1 were utilized in subsequent community analyses so that differences in community patterns were not due to differences in visibility.



215 **Table 1: Information for seven deployments conducted with the Nanolander *DOV BEEBE* including deployment dates, length,**
location, depth, environmental conditions for each deployment, total number of 20-second video samples available for the
community analysis, and camera and light performance for each data deployment. $[O_2] < 60 \mu\text{mol kg}^{-1}$ is defined as hypoxic, $[O_2] <$
 $22.5 \mu\text{mol kg}^{-1}$ is defined as severely hypoxic, and $\Omega_{\text{arag}} < 1$ and $\Omega_{\text{calc}} < 1$ are defined as undersaturated with respect to aragonite or
 220 **calcite, respectively. Mean and range O_2 percent saturation and pO_2 (kPa) for each deployment are provided in Supplement 1D.**
CV = coefficient of variation (i.e. the ratio of the standard deviation to the mean). pH_{est} is estimated pH, calculated using empirical
relationships from Alin et al. (2012).

	D200-LJ-1	D200-LJ-2	D100-DM-Fall	D200-DM	D300-DM	D400-DM	D100-DM-Spr
Dates	Aug 17-Sep 1, 2017	Sep 7-Sep 25, 2017	Sep 29-Nov 3, 2017	Nov 9-29, 2017	Dec 12, 2017 - Jan 5, 2018	Jan 23-Feb 8, 2018	Mar 8-Mar 29, 2018
Deployment Length	~15 days	~19 days	~35 days	~20 days	~24 days	~16 days	~21 days
Location	Scripps Coastal Reserve (32.87108° N, 117.26459° W)	Scripps Coastal Reserve (32.87108° N, 117.26457° W)	Del Mar Steeples Reef (32.93765° N, 117.31675° W)	Del Mar Steeples Reef (32.93762° N, 117.3254° W)	Del Mar Steeples Reef (32.93633° N, 117.33422° W)	Del Mar Steeples Reef (32.93105° N, 117.34875° W)	Del Mar Steeples Reef (32.93765° N, 117.31675° W)
Bottom Depth (m)	179	178	99	192	295	399	98
Mean Temp (°C)	10.07	9.88	11.10	9.51	8.39	7.42	9.80
Temp Range (°C)	9.72-10.43	9.45-10.44	10.35-12.26	8.94-10.21	7.99-8.77	6.97-7.89	9.39-10.30
CV Temp (%)	1.35	1.69	2.89	2.11	1.88	2.02	1.70
Mean $[O_2]$ ($\mu\text{mol kg}^{-1}$)	70.75	77.61	132.00	82.10	49.38	28.97	103.95
$[O_2]$ range ($\mu\text{mol kg}^{-1}$)	48.82-103.87	49.41-108.26	110.40-156.50	63.33-102.96	39.89-59.36	21.19-38.41	91.22-123.01
CV $[O_2]$ (%)	13.72	12.92	5.07	9.82	7.02	10.20	5.72
Mean pH_{est}	7.646	7.655	7.759	7.658	7.594	7.553	7.70
pH_{est} Range	7.607-7.704	7.605-7.711	7.713-7.814	7.625-7.699	7.575-7.613	7.538-7.572	7.671-7.732
CV pH_{est} (%)	0.22	0.23	0.2	0.19	0.09	0.08	0.15
Conditions hypoxic (% time)	12.64%	1.88%	0%	0%	100%	100%	0%
Conditions severely hypoxic (% time)	0%	0%	0%	0%	0%	1.12%	0%
Conditions undersaturated (aragonite) (% time)	99.65%	99.77%	0%	100%	100%	100%	92.80%
Conditions undersaturated (calcite) (% time)	0%	0%	0%	0%	0%	97.30%	0%
Number of 20-sec video samples for analysis	N/A	1009	876	1012	406	594	396
Number of video samples with good visibility	N/A	1009	876	656	6	594	396
Amount of time before lights first failed (h)	N/A	5.61	4.77	5.63	2.26	3.30	2.21

225 Non-metric multidimensional scaling was used to assess community-level differences across deployments. The R package “vegan” (Oksanen et al. 2017) was used for nMDS analysis and a Wisconsin double standardization was performed and counts were transformed using a square-root transformation. These standardizations are frequently used when working with datasets with high count values and have been found to improve nMDS results (Oksanen et al. 2017). Bray-Curtis dissimilarity was used as the input and community dissimilarities were mapped onto ordination space for the nMDS analysis.



Rare species (<8 observations across all deployment samples) and video samples with only one animal observation were removed from the community matrix, resulting in a total number of 3357 video samples and 43 unique species included in
230 the community analysis.

Since fishes are typically less hypoxia-tolerant than invertebrates (Vaquer-Sunyer and Duarte 2008), we hypothesized there would be a shift from a fish- to an invertebrate-dominated seafloor community that correlated with decreasing oxygen conditions. Samples from all deployments were categorized as “Fish Dominant”, “Equal”, or “Invertebrate Dominated” based on if there were more fishes or more invertebrates observed in each 20-second video
235 sample. These categories were then projected onto ordination space and superimposed with oxygen contours using the ordisurf function in “vegan”.

Since low oxygen conditions have been found to depress fish diversity (Gallo and Levin 2016), rarefaction diversity and fish species accumulation curves relative to number of video samples were examined to look at differences in fish diversity across deployments. We selected rarefaction diversity since the number of video samples differed across
240 deployments (Table 1). Only video samples in which fish were present were included in the calculation of the species accumulation curves.

To test the ability of the Nanolander to capture short-term responses in seafloor communities, we selected two deployments that had high environmental variability (D200-LJ-2 and D200-DM). For these deployments, samples were grouped in day (6:00 am-5:59 pm PST) and night (6:00 pm-5:59 am PST) categories and oxygen categories (“High”, “Intermediate”, and “Low”). Oxygen categories were determined separately for each deployment based on the deployment
245 time series, and were selected to showcase extremes: “High” samples represented the highest 10% of observed oxygen conditions, and “Low” samples the lowest 10% of observed oxygen conditions for the deployment. All other samples were categorized as “Intermediate.” An nMDS analysis was performed to look at differences in communities in relation to diurnal patterns and oxygen conditions within the timeframe of a single deployment. Rare species with fewer than 3 observations
250 across the deployment time series were removed from the community matrices, resulting in a community matrix with 844 video samples and 19 species for D200-LJ-1 and 645 video samples and 17 species for D200-DM. These were used in the nMDS analysis.

3 Results

3.1 Nanolander performance

255 *DOV BEEBE* was found to be a reliable platform for deployment, recovery, and data collection. Small boats were used for deployment and recovery (Fig. 1D and E) and *DOV BEEBE* was easily transported by lab cart or car. The Nanolander framework was robust and showed very few signs of wear following multiple deployments. Spheres showed no signs of leakage or vacuum loss, and acoustic communication worked well during all deployments.



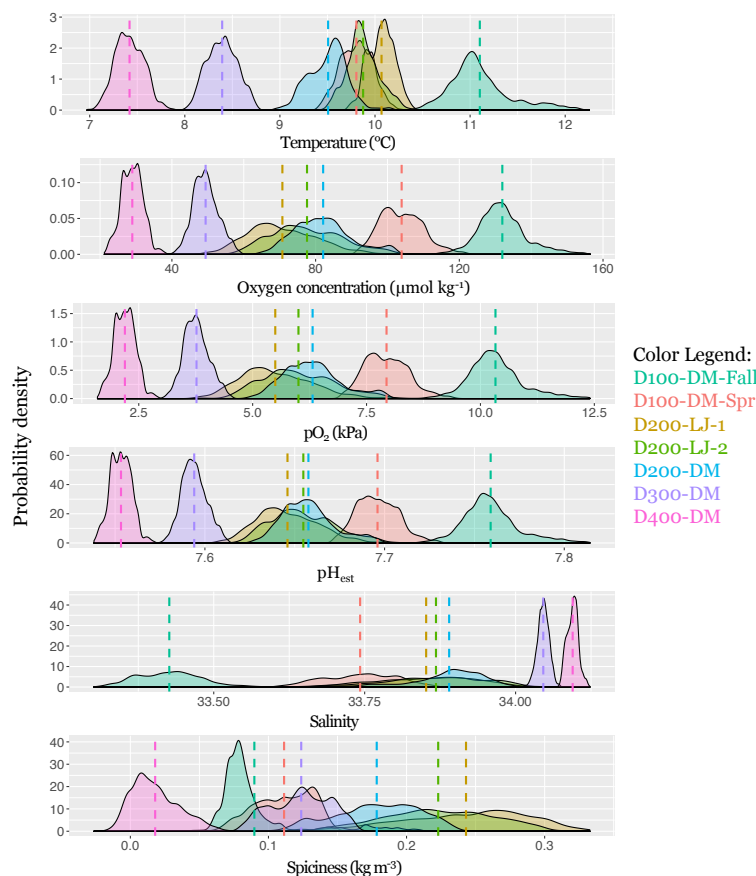
Memory and power capacity often limit deployment times for long-term, deep-sea deployments. We found that the
260 main limitation to deployment duration was the power requirement for the LED lights. As opposed to 8 hours of estimated
LED performance time, field performance ranged from 2.2 to 6.6 hours total time, which meant that the total time of
biological data collection was shortened and ranged from 5.5 to 16.5 days, respectively (Table 1). Memory and power were
not issues for the camera system; the 128 GB micro SD card was cleared and the battery pack was fully recharged following
each deployment. Video quality was high enough to allow species-level identifications and the light from the LEDs was
265 sufficient to light the field of view (Fig. 1F and G). The SeaBird MicroCAT-ODO also performed without any issues and
had sufficient battery and memory capacity for all deployments. Detailed descriptions of Nanolander performance can be
found in Gallo (2018).

3.2 Characteristics and drivers of oxygen variability across short time-scales

Natural variability of environmental parameters was assessed from time series data collected during each
270 deployment and compared across depths (100, 200, 300, and 400 m), and season (fall compared to spring). Means and ranges
for temperature, oxygen, salinity, and pH_{est} for each deployment were determined (Table 1). At ~100 m, conditions were
never hypoxic (i.e. $< 60 \mu\text{mol kg}^{-1}$), although the mean oxygen concentration was significantly lower during the spring
upwelling season deployment (D100-DM-Spr, mean $\text{O}_2 = 104 \mu\text{mol kg}^{-1}$), compared to the fall deployment when upwelling
was relaxed (D100-DM-Fall, mean $\text{O}_2 = 132 \mu\text{mol kg}^{-1}$) (ANOVA, $p < 0.001$). pH_{est} was also lower during the spring
275 deployment (D100-DM-Spr, mean $\text{pH}_{\text{est}} = 7.696$) than during the fall deployment at ~100 m (D100-DM-Fall, mean $\text{pH}_{\text{est}} =$
7.759) (ANOVA, $p < 0.001$), and temperatures were on average 1.3°C colder, consistent with upwelling conditions (Table 1,
Fig. 2). While conditions were never undersaturated with respect to aragonite ($\Omega_{\text{arag}} < 1$) during the fall deployment, during
the spring deployment, conditions were undersaturated ~93% of the time (Table 1).

At ~200 m, hypoxic conditions ($\text{O}_2 < 60 \mu\text{mol kg}^{-1}$) were encountered, however conditions were only hypoxic for
280 relatively short portions of the deployment (~13% for D200-LJ-1, ~2% for D200-LJ-2, and never hypoxic for D200-DM)
(Table 1). These results, if characteristic of other years, suggest that at depths around 200 m, benthic organisms are
periodically exposed to hypoxic conditions in the late summer and fall, but these conditions are not continuous. Conditions
were almost always undersaturated with respect to aragonite ($\Omega_{\text{arag}} < 1$) (Table 1).

At ~300 m (D300-DM) and ~400 m (D400-DM), mean temperatures were colder, and mean oxygen and pH_{est}
285 conditions were lower (Table 1, Fig. 2). At both depths, conditions were continuously hypoxic, and at 400 m (D400-DM)
conditions were severely hypoxic (i.e. $\text{O}_2 < 22.5 \mu\text{mol kg}^{-1}$) for ~1% of the time-series (Table 1). Both D300-DM and D400-
DM were conducted during the fall/winter, when upwelling conditions are relaxed, therefore deployments likely captured the
less extreme (higher oxygen, higher pH) conditions. This suggests that at ~300 m, seafloor communities are continuously
exposed to hypoxic conditions throughout the year, and at ~400 m communities are periodically exposed to OMZ conditions.
290 At ~300 m, the seawater is undersaturated with respect to aragonite ($\Omega_{\text{arag}} < 1$) but not calcite, whereas at ~400 m, conditions
are also undersaturated with respect to calcite ($\Omega_{\text{calc}} < 1$) for most of the deployment (Table 1).



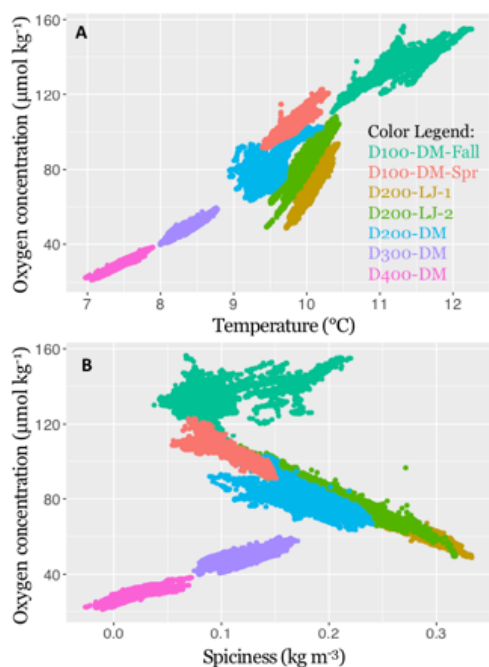
295 **Figure 2: Mean and variance of near-seafloor temperature, oxygen concentration, oxygen partial pressure, pH_{est}, salinity, and spiciness. The probability density of data collected for each deployment is shown, with the color of the data distributions corresponding to each deployment (as indicated in the color legend). The mean is indicated with a dotted line in the same color and exact values are given in Table 1. pH_{est} is estimated pH, calculated using empirical relationships from Alin et al. (2012). Sampling dates for each deployment are given in Table 1.**

300 While we expected that O₂ variability would decrease with depth, instead we found that the greatest variance in oxygen conditions over these short time-scales was observed at ~200 m (Table 1). All three deployments from ~200 m showed broad probability density distributions of environmental conditions (Fig. 2) and large ranges in oxygen and pH_{est} for the deployment period (Table 1). The coefficient of variation (CV) for oxygen at ~200 m was twice higher than for the ~100 m deployments (Table 1). While deployments at ~300 m (D300-DM) and ~400 m (D400-DM) had much narrower probability density distributions of environmental conditions (Fig. 2), the ranges in oxygen and pH_{est} at ~400 m were only slightly smaller than at ~300 m (Table 1). The CV for oxygen was higher at ~400 m (10.20%) compared to ~300 m (7.02%)



305 (Table 1). Temperature did not exhibit the same pattern of variability as oxygen, with the highest variance (CV) observed during D100-DM-Fall (~100 m) (Table 1). Variance in pH_{est} (CV) was almost twice higher at shallower depths (< 200 m), than at ~300 or ~400 m (Table 1).

Using a spectral analysis, we found that the dominant frequency underlying oxygen variability for all deployments was close to the semidiurnal tidal period (~12.4 hrs) (Supplement 1A). Deconstructed time series also showed a clear diurnal and semi-diurnal signal at all depths (Supplement 1B). Thus, oxygen variability on the outer shelf and upper slope is mainly driven by tides. The relative amplitude of the dominant signal in the periodogram decreases with increasing depth, suggesting that the strength of the tidal signal weakens with depth. Oxygen conditions tend to increase during ebb tide as the tide retreats, and decrease during flood tide as the tide rises (Supplement 1C).



315 **Figure 3:** 2017-2018 near-bottom dissolved oxygen concentration in the Southern California Bight shown in relation to
320 temperature and spiciness. Data points represent samples taken every five minutes with the SBE MicroCAT-ODO sensor during
the seven deployments. Deployments are distinguished by color, as indicated in the color legend. Sampling dates for each
deployment are given in Table 1.

Oxygen concentration was found to be significantly positively correlated with temperature for all deployments (LR, $p < 0.001$), however, the explanatory power of the regressions differed across depths (100, 200, 300, and 400 m) and the slopes of the regressions differed between locations (Scripps Reserve and Del Mar Steeples Reef). At depths deeper than 200 m, there was less variance around the linear trend in oxygen. The highest amount of oxygen variance explained by the linear



regression with temperature was found for D400-DM (~400 m, $R^2 = 0.90$), and the lowest amount for D200-DM (~200 m, $R^2 = 0.41$). The two deployments conducted near the Scripps Reserve (D200-LJ-1 and D200-LJ-2) had steeper slopes (Fig. 325 3) than deployments on the Del Mar Steeples Reef (D100-DM-Fall, D200-DM, D300-DM, D400-DM, D100-DM-Spr), which may be related to bathymetric differences of the sites. Deployments near the Scripps Reserve were in a narrow, deep tendril of the Scripps canyon system, which is surrounded by shallower bathymetry, while the Del Mar deployments were on a gradually sloping margin.

Oxygen was significantly correlated with spiciness for all deployments (LR, $p < 0.001$), however, the slopes and 330 explanatory power of this relationship differed across depths (100, 200, 300, and 400 m) and season (fall and spring) (Fig. 3). D100-DM-Fall and D100-DM-Spr were conducted at the same location at ~100 m, but during fall and spring, respectively, and exhibited differing relationships between oxygen and spiciness (Fig. 3). In the fall, the relationship between spiciness and oxygen at ~100 m was weak and positive with low explanatory power ($R^2 = 0.31$). In contrast, during spring, dissolved oxygen was negatively correlated with spiciness, and the linear fit had high explanatory power ($R^2 = 0.81$). At 335 ~200 m (D200-LJ-1, D200-LJ-2, D200-DM), spiciness and oxygen concentration were also negatively correlated, with high explanatory power for the linear fits ($R^2 = 0.98, 0.92, \text{ and } 0.61$, respectively) (Fig. 3). At deeper depths (~300 and 400 m), the relationship between spiciness and oxygen was significant (LR, $p < 0.001$), but the correlation was positive with high explanatory power of the linear fit (D300-DM $R^2 = 0.61$, D400-DM $R^2 = 0.68$).

3.3 Seafloor community differences and relationship to oxygen conditions

340 Community data were collected using the camera system during six deployments (Table 1), representing a total of 4,293 20-second videos that were annotated for organismal observations. Unexpected differences in visibility were observed across deployments. Clear conditions were present for deployments D200-LJ-2, D100-DM-Fall, D400-DM and D100-DM-Spr. During D200-DM at Del Mar Steeples Reef, visibility deteriorated throughout the deployment. The following deployment, D300-DM, which was at ~300 m at Del Mar Steeples Reef, had very poor visibility. For D300-DM, less than 345 2% of samples had good visibility, 78% had impaired visibility, and 20% had severely impaired visibility due to high sediment turbidity.

The community at the Del Mar Steeples Reef at ~100 m (D100-DM-Fall and D100-DM-Spr) was characterized by high numbers of rockfish (*Sebastes spp.*), especially halfbanded rockfish (*S. semicinctus*), but also included rarer rockfish species such as the flag (*S. rubrivinctus*), Bocaccio (*S. paucispinis*), rosy (*S. rosaceus*), and greenstriped rockfish (*S. 350 elongatus*). Other fishes included the pink surfperch, *Zanobius rosaceus*, combfish, *Zaniolepis spp.*, and the spotted cusk-eel, *Chilara taylori*. Invertebrates were not abundant, but included an unidentified gastropod, the tuna crab, *Pleuroncodes planipes*, a yellow coral, as well as others. Except for the singular yellow coral, all other invertebrates were mobile. Seafloor communities for D100-DM-Fall and D100-DM-Spr show high similarity, but are distinct from most other deployments (Fig. 4A).



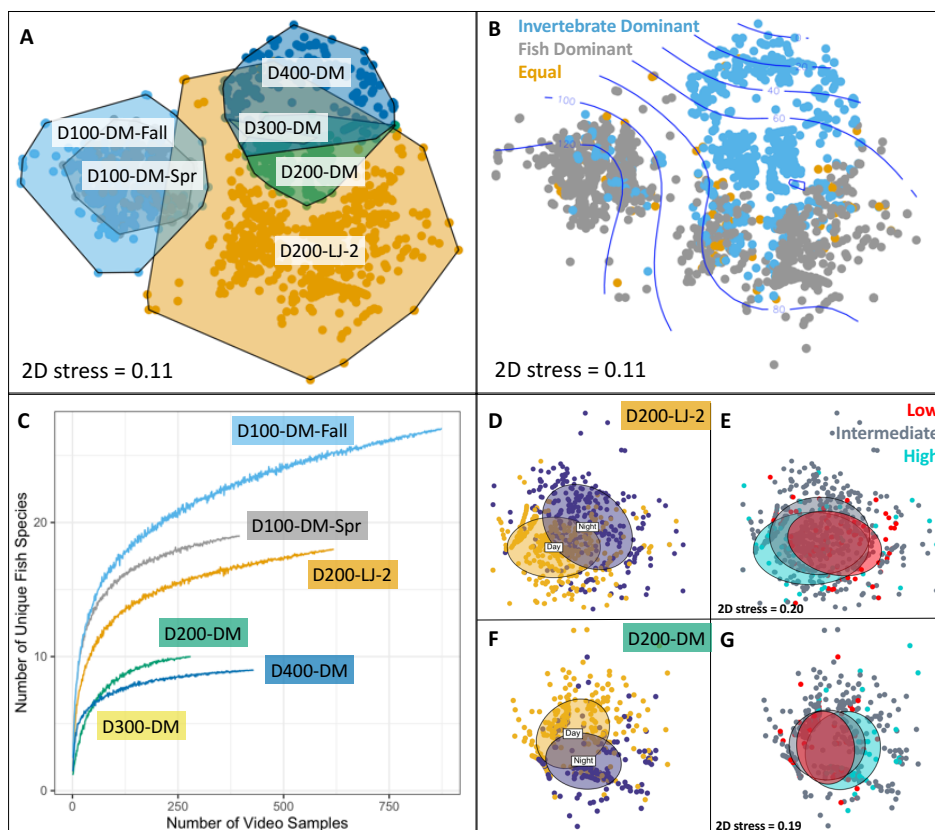
355 Deployments D200-LJ-2 and D200-DM were in different locations (Table 1), and the communities observed were
very different despite the similar depth and environmental conditions (Fig. 4A). The community at D200-LJ-2 included
eelpouts (*Lycodes spp.*), cusk-eels (*C. taylori*), lizardfish (*Synodus lucioceps*), and crabs (*Cancer spp.*), as well as, more
typical deep-water species such as Dover sole (*Microstomus pacificus*), chimaeras (*Hydrolagus colliei*), and dogface witch-
eels (*Faciolella equatorialis*). In contrast, rockfish (*Sebastes spp.*), combfish (*Zaniolepis spp.*), and Pacific sanddab
360 (*Citharichthys sordidus*) were commonly observed during D200-DM, and the community was dominated by tuna crabs (*P.*
planipes) and pink urchins (*S. fragilis*) which were present in high abundances. In contrast, during D200-LJ-2, no pink
urchins were observed, and tuna crabs were less abundant. Spot prawns (*Pandalus platyceros*) were common community
members observed during both D200-LJ-2 and D200-DM, but were not observed during any other deployments.

Only one deployment each was conducted at the two deeper depths (~300 m and 400 m) and both deployments
365 were near the Del Mar Steeples Reef. Due to poor visibility, the bottom was only visible in a few samples from D300-DM.
From these, it appeared that the community was dominated by tuna crabs (*P. planipes*) and pink urchins (*S. fragilis*), though
in lower abundances than at D200-DM. Fish were rarely observed, but included Pacific hake (*Merluccius productus*),
rockfish (*Sebastes spp.*), Pacific hagfish (*E. stoutii*), and hundred-fathom codling (*Physiculus rastrelliger*). D300-DM
showed similarity to seafloor communities observed during D200-DM and D400-DM (Fig. 4A).

370 D400-DM represented the deepest deployment (~400 m) and had excellent visibility. The community was
dominated by pink urchins (*S. fragilis*), but these were present in lower abundances than at D200-DM. Low numbers of tuna
crabs (*P. planipes*) were also present. Fish were rare, but the common fishes observed were Pacific hagfish (*E. stoutii*),
blacktip poacher (*Xeneretmus latifrons*), dogface witch eels (*F. equatorialis*), Dover sole (*M. pacificus*), and shortspine
thornyhead (*Sebastolobus alascanus*). Both fish and invertebrates were less active and showed less movement in D400-DM
375 than at shallower deployments.

We also looked at a community-level metric in relation to environmental oxygen conditions: community dominance
by invertebrates or fishes. We hypothesized that higher-oxygen conditions would be characterized by fish dominance,
compared to lower-oxygen conditions, which would be characterized by invertebrate dominance. Deployments D200-DM,
D300-DM, and D400-DM were characterized by invertebrate dominance for either all or most (>98%) samples. In contrast,
380 D200-LJ-2, D100-DM-Fall, and D100-DM-Spr were characterized by mixed communities, with fish-dominated
communities more characteristic for D100-DM-Fall and D100-DM-Spr. In general, fish-dominated communities were more
characteristic of higher-oxygen conditions when looking across all deployments (Fig. 4B), but we do not know if this is due
to oxygen or other environmental covariates.

We were also able to examine differences in fish diversity across deployments using the Nanolander video samples.
385 Species accumulations curves show differences in fish species rarefaction diversity across deployments, with D100-DM-Fall
having the highest number of observed fish species, followed by D100-DM-Spr, D200-LJ-2, D200-DM, and D400-DM (Fig.
4C). The decline in rarefaction diversity between D100-DM-Fall and D100-DM-Spr may be related to changes in
environmental conditions between fall and spring, since the location is the same (Table 1).



390 **Figure 4:** Seafloor community analyses using *DOV BEEBE* video samples. A) Non-metric multidimensional scaling plot showing
 seafloor community similarity across six deployments. Points represent Bray-Curtis similarity of square-root transformed counts
 of animals observed in each 20-second video sample ($n = 3357$) from each deployment ($n = 6$). Points are color-coded by
 deployment and a convex hull demarcates each deployment community. B) The same nMDS as in A) but points are color-coded by
 395 whether the seafloor community for each 20-second video sample was dominated by invertebrates (blue), vertebrates (gray), or an
 equal proportion of vertebrates and invertebrates (gold). Blue contours indicate relationship with oxygen concentration ($\mu\text{mol kg}^{-1}$).
 C) Species accumulation curves showing differences in fish rarefaction diversity across deployments. D-G) Non-metric
 multidimensional scaling plots showing differences in seafloor community composition as a function of day versus night (D, F) and
 400 oxygen conditions (E, G) for two deployments: D200-LJ-2 (D, E) and D200-DM (F, G). In D) and F) yellow points represent
 daytime samples (6:00 AM – 5:59 PM) and purple points represent nighttime samples (6:00 PM – 5:59 AM). In E) and G), low
 (red) and high (blue) oxygen conditions represent the lowest and highest 10th percentile of oxygen conditions encountered during
 each deployment time series. Ellipses represent grouping by category and show 50% confidence limits. 2D stress is the same for D)
 and E) and for F) and G). See Table 1 for camera deployment details.

We were also able to examine community-level changes within deployments to look at day/night differences in
 seafloor communities and to examine if seafloor communities respond to high-frequency oxygen variability. D200-LJ-2 and
 405 D200-DM, which exhibited the highest oxygen variability and each had ~14-day time series of camera samples (Table 1,
 Fig. 2), were selected for further analysis. Clear diurnal differences were observed for both deployments (Fig. 4D, F),



showing that at 200 m, communities are intimately linked to diurnal rhythms. Daytime communities were characterized by more combfish (*Zaniolepis spp.*), hake (*M. productus*), small pelagic fish (*Engraulis mordax*), blacktip poachers (*X. latifrons*), and crabs (*Cancer spp.*), while nighttime communities were characterized by more lizardfish (*S. lucioceps*), spot
410 prawns (*P. platyceros*), chimaeras (*H. colliei*), and hagfish (*E. stoutii*). Tuna crabs (*P. planipes*) and pink urchins (*S. fragilis*) showed no diurnal differences.

In contrast to clear diurnal differences, seafloor communities showed little evidence of responsiveness to changing oxygen conditions during the two deployments examined, however, some community-level differences do emerge when examining the highest and lowest oxygen conditions that were encountered during the deployment time series (Fig 4E, G).
415 At ~200 m, crabs (*Cancer spp.*), spot prawns (*P. platyceros*), and lizardfish (*S. lucioceps*) were more common community members during the high oxygen extremes while tuna crabs (*P. planipes*) and Dover sole (*M. pacificus*) were more common during low oxygen extremes. For both deployments, the video time series lasted ~14 days, and a longer time series may show more community-level differentiation in relation to oxygen extremes. Overall, our results show that at short-timescales (2 weeks or less), seafloor communities responded to diurnal differences more than to high-frequency oxygen variability.

420 4 Discussion

The California Current System is expected to experience the impacts of hypoxia and ocean acidification on seafloor communities sooner than other regions (Alin et al. 2012) because upwelling brings deep, oxygen-poor, and CO₂-rich waters into nearshore ecosystems along the US West Coast (Feely et al. 2008). Species in the SCB region may be particularly vulnerable to deoxygenation-induced habitat compression because the depth of the 22.5 μmol kg⁻¹ oxygen boundary (i.e.
425 upper OMZ boundary) occurs at a shallower depth here than in northern California, Oregon, and Washington (Helly and Levin 2004, Moffitt et al. 2015). This study shows that even during the relaxed upwelling season, seafloor communities at ~400 m can be periodically exposed to OMZ conditions, communities at ~300 m are continuously exposed to hypoxic conditions, and communities at ~200 m are periodically exposed to hypoxic conditions. Input of Pacific Equatorial Water (PEW), which is brought up by the California Undercurrent, is key to determining near-seafloor oxygen conditions at ~200
430 m, and in the spring, PEW upwells to 100 m leading to lower oxygen conditions. In contrast, at deeper depths (~300 and 400 m), added input of PEW increases oxygen conditions. Seafloor communities differ across the sampled environmental conditions, with communities living in lower-oxygen areas characterized by invertebrate dominance and decreased fish diversity.

4.1 Comparing short-term variability of oxygen to long-term trends

435 To compare the magnitude of natural O₂ variability over short time scales with reported trends of longer-term deoxygenation, we compared our results with the annual rates of oxygen loss reported for the SCB nearshore region (Bograd et al. 2008). From our data, we see that at 100 m, at daily time scales, semidiurnal and diurnal variability exposes benthic



communities to $\sim 4\text{--}7 \mu\text{mol kg}^{-1}$ differences in oxygen conditions (Supplement 1B). Across, weekly time-scales, benthic communities experience a range of oxygen conditions of $\sim 32 \mu\text{mol kg}^{-1}$ (D100-DM-Spr) – $46 \mu\text{mol kg}^{-1}$ (D100-DM-Fall).
440 Between the fall and spring deployments, mean oxygen conditions decreased from 132 to $104 \mu\text{mol kg}^{-1}$ (Table 1). Even larger extreme event-based decreases in oxygen have been reported near our study site at the Del Mar mooring at ~ 100 m (Nam et al. 2015).

The rate of reported oxygen loss at ~ 100 m from 1984 to 2006 was $1.25\text{--}1.5 \mu\text{mol kg}^{-1} \text{year}^{-1}$ (Bograd et al. 2008). Over a period of ~ 20 years, this rate of oxygen loss equates to the seasonal difference at 100 m between the spring upwelling
445 season and the fall. If this rate of oxygen loss continues, in 20 years, fall conditions would resemble current spring conditions, while spring conditions would be even lower ($\sim 75 \mu\text{mol kg}^{-1}$ mean $[\text{O}_2]$), potentially exposing communities at ~ 100 m to periodic hypoxic conditions, to which they are not currently exposed.

At ~ 200 m, oxygen, temperature, and pH exhibited high variability (Fig. 2), greater at times than the variability observed at 100 m. Communities at these depths experience $10\text{--}12 \mu\text{mol kg}^{-1}$ differences in oxygen at semidiurnal and
450 diurnal time-scales (Supplement 1B), and over weekly timescales communities experience high variability around the mean (Table 1, Fig. 2). These depths have experienced an oxygen decline of $1\text{--}1.25 \mu\text{mol kg}^{-1} \text{year}^{-1}$ loss (Bograd et al. 2008), suggesting that if this same rate of oxygen decline continues, the mean oxygen conditions at these depths (which ranged from $\sim 70\text{--}82 \mu\text{mol kg}^{-1}$ from our data) will be continuously hypoxic in 10–20 years. Currently, communities are exposed to hypoxic conditions during the fall for $<15\%$ of the time in our time series (Table 1), but may experience hypoxic conditions
455 more frequently in the spring.

If mean conditions do become hypoxic at 200 m, the high variability we observed in environmental conditions at this depth may be advantageous to hypoxia intolerant members of the benthic community. Frieder et al. (2014) concluded that high-frequency pH variability was an underappreciated source of pH-stress alleviation for invertebrates that were sensitive to low pH conditions. In a hypoxic fjord, slender sole, *Lyopsetta exilis*, were also observed living under mean
460 oxygen conditions that were lower than their critical oxygen threshold (P_{crit}), apparently due to the presence of oxygen variability around the mean (Chu et al. 2018). High-frequency variability of environmental conditions could help buffer the negative effects of changing mean environmental conditions for benthic communities at 200 m.

The greatest relative long-term changes in oxygen in the SCB have been reported at 300 m and represent an absolute change of $0.5\text{--}0.75 \mu\text{mol kg}^{-1} \text{year}^{-1}$ (Bograd et al. 2008). In contrast to the high environmental variability observed
465 at 200 m, variability at 300 m was reduced and more similar to variability at 400 m (Fig. 2, Table 1). At daily timescales, a tidal signal still influenced oxygen conditions, which ranged $\sim 2 \mu\text{mol kg}^{-1}$ (Supplement 1B). At weekly time scales, the range of oxygen conditions was $\sim 19 \mu\text{mol kg}^{-1}$, or $\sim 39\%$ of mean conditions at this depth ($49.38 \mu\text{mol kg}^{-1}$). Conditions at 300 m were always hypoxic, so these depths likely do not provide suitable habitat for hypoxia intolerant species under current conditions.

470 We note that 300 m is an interesting depth which may be at an important boundary between two different water masses. The correlation between spiciness and oxygen concentration is negative at 200 m (indicative of high input of PEW),



and then positive at 300 m (Fig. 3). Since changes in the volume of PEW have been implicated in the decreases in oxygen observed in the SCB (Booth et al. 2014, Bograd et al. 2015), it is worthwhile to note that increased input of this water mass could have a nonlinear effect on oxygen conditions in this area: increasing oxygen conditions at deeper depths, while
475 decreasing them at shallower depths. The mechanism giving rise to the high turbidity observed at this depth also remains a mystery. High turbidity conditions have also been observed during two separate ROV dives at ~340 m off Point Loma (unpublished), suggesting high turbidity conditions may be the norm at these depths on the upper slope in the SCB.

At 400 m, absolute variability of oxygen conditions was only slightly lower than that at 300 m (Table 1), but since the mean conditions were ~20 $\mu\text{mol kg}^{-1}$ lower at 400 m, the relative variability in oxygen conditions was higher. At daily
480 timescales, oxygen varied ~2 $\mu\text{mol kg}^{-1}$ with the tides, and at weekly timescales, we observed a range of 17 $\mu\text{mol kg}^{-1}$, which represented 59% of the mean. Therefore, the amount of oxygen variability relative to the mean at 400 m, was similar to that at 200 m, suggesting that variability in oxygen conditions may provide some reprieve to benthic communities at this depth from low mean oxygen conditions. At this depth, we recorded severely hypoxic conditions ($\text{O}_2 < 22.5 \mu\text{mol kg}^{-1}$) for ~1% of the deployment time (Table 1), suggesting that even though this community is above the depth frequently associated with the
485 upper boundary of the OMZ (450 m), it is still periodically exposed to OMZ conditions. High spatial resolution-sampling of the eastern tropical North Pacific OMZ documents considerable submesoscale oxygen variability with better oxygenated holes (Wishner et al. 2019); such patchiness would not be unexpected off southern California. Oxygen decreases of 0.25-0.5 $\mu\text{mol kg}^{-1} \text{ year}^{-1}$ have been reported for depths of 400 m (Bograd et al. 2008), and if these trends continue, in 13-26 years, this depth zone may become the upper boundary of the OMZ.

490 While we have related our results to reported trends for the SCB from Bograd et al. (2008), it is unclear if these trends will continue, since multidecadal oxygen trends associated with the Pacific Decadal Oscillation (PDO) may reverse (McClatchie et al. 2010). In the 1950s and 1960s, oxygen levels were also very low in the SCB, and McClatchie et al. (2010) note that at ~250 m, conditions were as low or lower than those reported in the early 2000s. Additionally, projections for the California Current System suggest winds near the equatorward boundary may weaken as winds strengthen in the northern
495 region (Rykaczewski et al. 2016).

4.2 Observations of community responses to high-frequency environmental variability

Using *DOV BEEBE*, we were able to describe outer shelf and upper slope assemblages and examine if and how the seafloor community responds to O_2 variability at short timescales (daily, weekly, seasonal) in terms of community composition and diversity. Unexpectedly, we did not see strong evidence of seafloor community-level responses to daily and
500 weekly oxygen variability. Seasonal differences were observed for D100-DM-Fall and D100-DM-Spr, but it is unclear if these were driven by oxygen, other upwelling-related environmental covariates such as temperature, pH, and productivity, or seasonal behavioral shifts associated with spawning or other activities.

Pronounced and rapid (< 2 week) community-level responses to hypoxia may occur in certain cases. For example, the Del Mar mooring has recorded strong event-based changes in dissolved oxygen (Nam et al. 2015) where oxygen rapidly



505 increased or decreased over a short time-period (< 2 weeks). Rapid changes such as these that are outside of the typical regime of oxygen variability may lead to more immediate community responses. Unfortunately, we did not capture any such events during our deployments. Second, community-level responses may be observed if the mean environmental conditions are close to a critical threshold for a species that is dominant in the community. Spot prawn (*P. platyceros*) and crabs (*Cancer spp.*) were more strongly associated with the highest oxygen conditions during the D200-LJ-2 and D200-DM
510 deployments, suggesting the oxygen conditions may be close to a critical threshold for these species. Tolerances to hypoxia are species-specific, with high intraspecies variability, so longer time series may better detect community-level changes. Given that we saw limited community-level responses at daily and weekly timescales, future deployments could sample less frequently (one camera sample taken every hour or every two hours) but over longer time periods (~4-8 weeks) to examine community-level responses to environmental variability.

515 The lack of community-level response to diurnal and weekly oxygen variability seen in our data may not be surprising given that animals have several ways that they can respond to stressful conditions, which would not affect community-level abundance, diversity, or composition patterns. For example, fish can become less active and reduce metabolic demands (Richards 2009, 2010), or can decrease feeding behavior (Wu 2002, Nilsson 2010) during periodic hypoxia. We observed that animals were less active in the deeper deployments, but it is unclear if this is due to the lower
520 oxygen conditions or other environmental covariates.

4.3 A global array of deep-sea landers

Ocean deoxygenation is a global concern, with changes in oxygen conditions potentially impairing the productivity of continental shelves and margins that support important ecosystem services and fisheries. Many of the areas where large decreases in oxygen have been observed occur in developing countries, such as along the western and eastern coast of Africa
525 (Schmidtko et al. 2017). Large oxygen losses have also been observed in the Arctic (Schmidtko et al. 2017), where the seafloor habitat is understudied.

Due to their compact design, small landers such as *DOV BEEBE* can provide easy access to nearshore, deep-sea ecosystems and could expand the capabilities of developed and developing countries to monitor and study environmental changes along their coastlines. We found that the Nanolander performed well and reliably over the course of the
530 deployments, and was a valuable tool for studying environmental variability, describing seafloor communities, and linking seafloor community responses to environmental forcing. One advantage of the Nanolander design is that it is modular and easy to modify to fit the scope of research that is needed, and other sensors and instruments can easily be added. For continental margins and seafloor habitats, a global array of Nanolandings, similar in scope to the Argo program, could be envisioned which would greatly expand our understanding of climate change impacts on seafloor communities.



535 **Code and data availability**

Code and data will be made available through Zenodo; code and dataset publication will be timed with manuscript acceptance and publication.

Author contribution

540 NG, LL, KH, and NW designed the research design; KH designed and built the nanolander; NG, KH, and HY carried out the field deployments; NG, HY, and AN performed the video annotation and data analysis; NG wrote the manuscript and all authors contributed to editing the manuscript.

Competing interests

Author Kevin Hardy is the owner of the company Global Ocean Design which currently sells nanolanders similar to *DOV BEEBE*.

545 **Acknowledgements**

This research was made possible through generous funding from several sources: the Mullin fellowship, Mildred E. Mathias Research Grant, the Edna B. Sussman Fellowship, the Mia J. Tegner Fellowship, Friends of the International Center Scholarship, the *DEEPSEA CHALLENGE* Expedition, the National Science Foundation Graduate Research Fellowship, and the Switzer Environmental Leadership Fellowship. Additionally, Global Ocean Design LLC provided internal R&D 550 resources. The Fisheries Society for the British Isles and the UCSD Graduate Student Association provided travel support to present these results at scientific meetings. This work would not have been possible without the support of a tremendous number of people who helped with Nanolander deployments and recoveries, especially Phil Zerofski, Brett Pickering, Rich Walsh, Jack Butler, Mo Sedaret, Lilly McCormick, Andrew Mehring, Ana Sirovic, Rebecca Cohen, Ashleigh Palinkas, Jen McWhorter. I am forever grateful for the support of Javier Vivanco and others at Baja Aqua Farms for recovering and 555 returning *DOV BEEBE* after it drifted into Mexican waters following an unsuccessful recovery. NG's Ph.D. committee members, B. Semmens, R. Norris, R. Burton, D. Victor, and R. Keeling, provided feedback on the research. NG is currently supported by a NOAA QUEST grant to B. Semmens.



References

- Alin, S. R., Feely, R. A., Dickson, A. G., Hernandez-Ayon, J. M., Juranek, L. W., Ohman, M. D., and Goericke, R.: Robust
560 empirical relationships for estimating the carbonate system in the southern California Current System and
application to CalCOFI hydrographic cruise data (2005-2011), *J. Geophys. Res.*, 117, C05033, 2012.
- Bay, R. A., and Palumbi, S. R.: Multilocus adaptation associated with heat resistance in reef-building corals, *Current
Biology*, 24, 2952-2956, 2014.
- Beebe, W.: *Half mile down*, Harcourt, Brace and Company, New York, 344 pp, 1934.
- 565 Bograd, S. J., Castro, C. G., Lorenzo, E. D., Palacios, D. M., Bailey, H., Gilly, W., and Chavez, F. P.: Oxygen declines and
the shoaling of the hypoxic boundary in the California Current, *Geophys. Res. Lett.*, 35, L12607, 2008.
- Bograd, S. J., Buil, M. P., Lorenzo, E. D., Castro, C. G., Schroeder, I. D., Goericke, R., Anderson, C. R., Benitez-Nelson, C.,
and Whitney, F. A.: Changes in source waters to the Southern California Bight, *Deep-Sea Res. II*, 112, 42-52, 2015.
- Booth, J. A. T., Woodson, C. B., Sutula, M., Micheli, F., Weisberg, S. B., Bograd, S. J., Steele, A., Schoen, J., and Crowder,
570 L. B.: Patterns and potential drivers of declining oxygen content along the southern California coast, *Limnol.
Oceanogr.* 59(4), 1127-1138, 2014.
- Chu, J. W. F., Curkan, C., and Tunnicliffe, V.: Drivers of temporal beta diversity of a benthic community in a seasonally
hypoxic fjord, *R. Soc. Open Sci.*, 5, 172284, 2018.
- Doya, C., Aguzzi, J., Pardo, M., Matabos, M., Company, J. B., Costa, C., Mihaly, S., and Canals, M.: Diel behavioral
575 rhythms in sablefish (*Anoplopoma fimbria*) and other benthic species, as recorded by the Deep-sea cabled
observatories in Barkley canyon (NEPTUNE-Canada), *Journal of Marine Systems*, 130, 69-78, 2014.
- Feely, R. A., Sabine, C. L., Hernandez-Ayon, J. M., Ianson, D., and Hales, B.: Evidence for upwelling of corrosive
“acidified” water onto the continental shelf, *Science*, 320, 1490-1492, 2008.
- Flament, P.: A state variable for characterizing water masses and their diffusive stability: Spiciness, *Prog. Oceanogr.*, 54,
580 493–501, 2002.
- Frieder, C. A., Gonzalez, J. P., Bockmon, E. E., Navarro, M. O., and Levin, L. A.: Can variable pH and low oxygen
moderate ocean acidification outcomes for mussel larvae?, *Glob. Change Biol.*, 20(3), 754-764, 2014.
- Frieder, C. A., Nam, S. H., Martz, T. R., and Levin, L. A.: High temporal and spatial variability of dissolved oxygen and pH
in a nearshore California kelp forest, *Biogeosciences* 9, 3917-3930, 2012.
- 585 Gallo, N. D.: Influence of ocean deoxygenation on demersal fish communities: Lessons from upwelling margins and oxygen
minimum zones, PhD. Dissertation, University of California, San Diego, 2018.
- Gallo, N. D., Cameron, J., Hardy, K., Fryer, P., Bartlett, D. H., and Levin, L. A.: Submersible- and lander-observed
community patterns in the Mariana and New Britain trenches: Influence of productivity and depth on epibenthic and
scavenging communities, *Deep-Sea Res. I*, 99, 119-133, 2015.



- 590 Gallo, N. D., and Levin, L. A.: Fish ecology and evolution in the world's oxygen minimum zones and implications of ocean deoxygenation, *Adv. Mar. Biol.*, 74, 117-198, 2016.
- Gilly, W. F., Beman, J. M., Litvin, S. Y., and Robison, B. H.: Oceanographic and biological effects of shoaling of the oxygen minimum zone, *Annu. Rev. Mar. Sci.*, 5, 393-420, 2013.
- Helly, J. J., and Levin, L. A.: Global distribution of naturally occurring marine hypoxia on continental margins, *Deep-Sea Res. I*, 51, 1159-1168, 2004.
- 595 Henson, S. A., Beaulieu, C., Ilyina, T., John, J. G., Long, M., Séférian, R., Tjiputra, J., and Sarmiento, J. L.: Rapid emergence of climate change in environmental drivers of marine ecosystems, *Nat. Commun.*, 8, 14682, 2017.
- Hofmann, A. F., Peltzer, E. T., Walz, P. M., and Brewer, P. G.: Hypoxia by degrees: establishing definitions for a changing ocean, *Deep-Sea Res. I*, 58, 1212-26, 2011a.
- 600 Hofmann, G. E., Smith, J. E., Johnson, K. S., Send, U., Levin, L. A., Micheli, F., Paytan, A., Price, N. N., Peterson, B., Takeshita, Y., Matson, P., Crook, E. D., Kroeker, K. J., Gambi, M. C., Rivest, E. B., Frieder, C. A., Yu, P. C., and Martz, T. R.: High-frequency dynamics of ocean pH: a multi-ecosystem comparison, *PLoS ONE* 6(12), e28983, 2011b.
- Jamieson, A. J.: Landers: Baited cameras and traps, In *Biological Sampling in the Deep Sea*, Ed. Malcolm R. Clark, Mireille Consalvey, and Ashley A. Rowden. John Wiley & Sons, Ltd, 2016.
- 605 Jamieson, A. J., Kilgallen, N. M., Rowden, A. A., Fujii, T., Horton, T., Lorz, A.-N., Kitazawa, K., and Priede, I. G.: Bait-attending fauna of the Kermadec Trench, SW Pacific Ocean: Evidence for an ecotone across the abyssal-hadal transition zone, *Deep-Sea Res. I*, 58, 49-62, 2011.
- Juniper, S. K., Matabos, M., Mihaly, S., Ajayamohan, R. S., Gervais, F., and Bui, A. O. V.: A year in Barkley Canyon: A time-series observatory study of mid-slope benthos and habitat dynamics using the NEPTUNE Canada network, *Deep-Sea Res. II*, 92, 114-123, 2013.
- 610 Keller, A. A., Ciannelli, L., Wakefield, W. W., Simon, V., Barth, J. A., and Pierce, S. D.: Occurrence of demersal fishes in relation to near-bottom oxygen levels within the California Current large marine ecosystem, *Fish. Oceanogr.* 24(2), 162-176, 2015.
- 615 Kelley, D., and Richards, C.: oce: Analysis of Oceanographic Data, R package version 0.9-22, <https://CRAN.R-project.org/package=oce>, 2017.
- Levin, L. A.: Manifestations, drivers, and emergence of open ocean deoxygenation, *Ann. Rev. Mar. Sci.*, 10, 229-260, 2018.
- Levin, L. A., Lieu, K.-K., Emeis, K.-C., Breitbart, D. L., Cloern, J., Deutsch, C., Giani, M., Goffart, A., Hofmann, E. E., Lachkar, Z., Limburg, K., Liu, S.-M., Montes, E., Naqvi, W., Ragueneau, O., Rabouille, C., Sarkar, S. K., Swaney, D. P., Wassman, P., and Wishner, K. F.: Comparative biogeochemistry-ecosystem-human interactions on dynamic continental margins, *Journal of Marine Systems*, 141, 3-17, 2015.
- 620 Long, M. C., Deutsch, C., and Ito, T. Finding forced trends in oceanic oxygen, *Glob. Biogeochem. Cycles*, 30, 381-397, 2016.



- Lynn, R. J., and Simpson, J. J.: The California Current System: The seasonal variability of its physical characteristics,
625 *Journal of Geophysical Research*, 92(C12), 12,947-12,966, 1987.
- Matabos, M., Aguzzi, J., Robert, K., Costa, C., Menesatti, P., Company, J. B., and Juniper, S. K.: Multi-parametric study of
behavioural modulation in demersal decapods at the VENUS cabled observatory in Saanich Inlet, British Columbia,
Canada, *Journal of Experimental Marine Biology and Ecology*, 401, 89-96, 2011.
- Matabos, M., Bui, A. O. V., Mihaly, S., Aguzzi, J., Juniper, S. K., and Ajayamohan, R. S.: High-frequency study of
630 epibenthic megafaunal community dynamics in Barkley Canyon: A multi-disciplinary approach using the
NEPTUNE Canada network, *Journal of Marine Systems*, 130, 56-68, 2014.
- Matabos, M., Tunnicliffe, V., Juniper, S. K., and Dean, C.: A year in hypoxia: Epibenthic community responses to severe
oxygen deficit at a subsea observatory in a coastal inlet, *PLoS ONE* 7(9), e45626, 2012.
- McClatchie, S., Goericke, R., Cosgrove, R., Auad, G., and Vetter, R.: Oxygen in the Southern California Bight:
635 Multidecadal trends and implications for demersal fisheries, *Geophysical Research Letters*, 37, L19602, 2010.
- Meinvielle, M., and Johnson, G. C.: Decadal water-property trends in the California Undercurrent with implications for
ocean acidification, *J. Geophys. Res. Oceans*, 118, 6687-6703, 2013.
- Moffitt, S. E., Moffitt, R. A., Sauthoff, W., Davis, C. V., Hewett, K., and Hill, T. M.: Paleoceanographic insights on recent
oxygen minimum zone expansion: lessons for modern oceanography, *PLoS ONE*, 10(1), e0115246, 2015.
- 640 Nam, S. H., and Send, U.: Direct evidence of deep water intrusions onto the continental shelf via surging internal tides, *J.*
Geophys. Res., 116, C05004, 2011.
- Nam, S., Takeshita, Y., Frieder, C. A., Martz, T., and Ballard, J.: Seasonal advection of Pacific Equatorial Water alters
oxygen and pH in the Southern California Bight. *J. Geophys. Res. Oceans* 120, doi:10.1002/2015JC010859, 2015.
- Nilsson, G. E.: Respiratory physiology of vertebrates: Life with and without oxygen, Cambridge University Press, New
645 York, 334 pp, 2010.
- Oksanen, J., Blanchet F. G., Friendly, M., Kindt, R., Legendre, P., McGlinn, D., Minchin, P. R., O'Hara, R. B., Simpson, G.
L., Solymos, P., Stevens, M. H. H., Szoecs E., Wagner, H.: vegan: Community Ecology Package, R package version
2.4-4, <https://CRAN.R-project.org/package=vegan>, 2017.
- Priede, I. G., and Bagley, P. M.: In situ studies on deep-sea demersal fishes using autonomous unmanned lander platforms,
650 *Oceanography and Marine Biology: an Annual Review*, 38, 357-392, 2000.
- Ren, A. S., Chai, F., Xue, H., Anderson, D. M., and Chavez, F. P.: A sixteen-year decline in dissolved oxygen in the Central
California Current, *Scientific Reports*, 8, 7290, 2018.
- Richards, J.: Metabolic and molecular responses of fish to hypoxia, *Fish Physiol.*, 27, 443-485, 2009.
- Richards, J.: Metabolic rate suppression as a mechanism for surviving environmental challenge in fish, *Prog. Mol. Subcell.*
655 *Biol.*, 49, 113-139, 2010.



- Rykaczewski, R. R., Dunne, J. P., Sydeman, W. J., Garcia-Reyes, M., Black, B. A., and Bograd, S. J.: Poleward displacement of coastal upwelling-favorable winds through the 21st century, *Geophys. Res. Lett.*, 42, 6424-6431, 2016.
- Schmidtko, S., Stramma, L., and Visbeck, M.: Decline in global oceanic oxygen content during the past five decades, *Nature*, 542, 335-339, 2017.
- 660 Send, U., and Nam, S.: Relaxation from upwelling: the effect on dissolved oxygen on the continental shelf, *J. Geophys. Res.*, 117, C04024, 2012.
- Vaquar-Sunyer, R., and Duarte, C. M.: Thresholds of hypoxia for marine biodiversity, *Proc. Natl. Acad. Sci. USA* 105, 15452-57, 2008.
- 665 Wishner, K. F., Seibel, B., and Outram, D.: Ocean deoxygenation and copepods: Coping with oxygen minimum zone variability, *Biogeosciences*, <https://doi.org/10.5194/bg-2019-394>, 2019.
- Wu, R. S. S.: Hypoxia: from molecular responses to ecosystem responses, *Mar. Pollut. Bull.*, 45, 35-45, 2002.